Wave Scattering in Periodic Media

Matthew Kehoe

Joint work with David Nicholls

February 15, 2022

Overview

Introduction: Maxwell's Equations

As a starting point we consider Maxwell's equations of macroscopic electromagnetism in the following form:

$$\nabla \times \underline{\mathbf{E}} = -\frac{\partial \underline{\mathbf{B}}}{\partial t}, \qquad \text{(Faraday's Law of Induction)} \tag{1a}$$

$$\nabla \times \underline{\mathbf{H}} = \mathbf{J} + \frac{\partial \underline{\mathbf{D}}}{\partial t}, \qquad \text{(Ampère's Law)} \tag{1b}$$

$$\nabla \cdot \underline{\mathbf{D}} = \rho, \qquad \text{(Gauss's Law)} \tag{1c}$$

$$\nabla \cdot \underline{\mathbf{B}} = 0. \qquad \text{(Gauss's Law for Magnetism)} \tag{1d}$$

These equations link the four (time dependent fields)

- $\underline{\mathbf{E}}=\underline{\mathbf{E}}$(x,y,z,t) is the electric field, $\underline{\mathbf{H}}=\underline{\mathbf{H}}$(x,y,z,t) is the magnetic field.
- $\underline{\mathbf{D}}=\underline{\mathbf{D}}$(x,y,z,t) is the electric displacement field.
- $\underline{\mathbf{B}}=\underline{\mathbf{B}}$(x,y,z,t) is the magnetic induction field.
- $\mathbf{J}$ is the current density, ρ is the charge density.

Linear, Isotropic, Homogeneous, Nonmagnetic Media

Limiting ourselves to linear, isotropic, homogeneous, nonmagnetic media, we specify the constitutive relations

$$\underline{\mathbf{D}} = \varepsilon_0 \varepsilon_r \underline{\mathbf{E}}, \tag{2a}$$

$$\underline{\mathbf{B}} = \mu_0 \mu_r \underline{\mathbf{H}}. \tag{2b}$$

- Permittivity (ε) is a constant which measures the resistance in forming an electric field through a medium.
- Permeability (μ) is a constant that measures a material's ability to form magnetic fields within it.
- ε_r is the relative permittivity.
- $\mu_r = 1$ is the relative permeability of the nonmagnetic medium.
- ε_0 and μ_0 are the electric permittivity and magnetic permeability of vacuum.

Two Fields: $\underline{\mathbf{E}}$ and $\underline{\mathbf{H}}$

Inserting (2) into (1) forms

$$\nabla \times \underline{\mathbf{E}} = -\mu_0 \partial_t \underline{\mathbf{H}}, \tag{3a}$$
$$\nabla \times \underline{\mathbf{H}} = \mathbf{J} + \varepsilon_0 \varepsilon_r \partial_t \underline{\mathbf{E}}, \tag{3b}$$
$$\nabla \cdot \underline{\mathbf{E}} = \rho / (\varepsilon_0 \varepsilon_r), \tag{3c}$$
$$\nabla \cdot \underline{\mathbf{H}} = 0. \tag{3d}$$

- As the material is isotropic, we can model the current density $\mathbf{J}$ and electric field $\underline{\mathbf{E}}$ through Ohm's law. This defines the linear relationship

$$\mathbf{J} = \sigma \underline{\mathbf{E}}$$

  where σ is a scalar representing the conductivity of the material.
- We further assume that there are no free charges (demanding $\rho \equiv 0$).

Time–Harmonic Maxwell's Equations

- Time domain methods and frequency domain methods are often used in computational electromagnetics. We will work in the frequency domain by removing the time dependence.
- To obtain time–harmonic solutions of the form

$$\underline{\mathbf{E}}(x,y,z,t) = \mathbf{E}(x,y,z)e^{-i\omega t}, \quad \underline{\mathbf{H}}(x,y,z,t) = \mathbf{H}(x,y,z)e^{-i\omega t}, \tag{4}$$

we insert (4) into (3) to obtain (under the assumption that $\rho \equiv 0$)

$$\nabla \times \mathbf{E} = i\omega\mu_0\mathbf{H}, \tag{5a}$$

$$\nabla \times \mathbf{H} = -i\omega\varepsilon_0\varepsilon\mathbf{E}, \tag{5b}$$

$$\nabla \cdot \mathbf{E} = 0, \tag{5c}$$

$$\nabla \cdot \mathbf{H} = 0. \tag{5d}$$

- Here, ε is the complex permittivity defined by $\varepsilon := \varepsilon_r + i\sigma/(\omega\varepsilon_0)$.

Two–Dimensional Simplifications

- In the context of grating structures, we choose an interface shaped by $z = g(x, y)$ where the normal is defined by $\mathbf{N} := (-\partial_x g, -\partial_y g, 1)^T$.
- To obtain two-dimensional solutions, we assume the grating shape is invariant in the y–direction:

$$z = g(x),$$

which implies that the interfacial normal becomes

$$\mathbf{N} = \begin{pmatrix} -\partial_x g \\ 0 \\ 1 \end{pmatrix}.$$

- For our boundary conditions, we enforce the tangential continuity of the fields $\mathbf{E}$ and $\mathbf{H}$ at every material interface:

$$\mathbf{N} \times \mathbf{E} = 0, \quad \mathbf{N} \times \mathbf{H} = 0.$$

Transverse Electric (TE) and Transverse Magnetic (TM) Polarization

- We further assume our incident radiation is aligned with the invariant grooves of our grating structure: implying that the radiation is both y–invariant and transversely aligned.
- Under this context, we may represent the incident field for Transverse Electric (TE) polarization by

$$\mathbf{E}^i = \mathbf{E}^i(x,z) = \mathbf{A} e^{i\alpha x - i\gamma z}, \quad \mathbf{A} = \begin{pmatrix} 0 \\ A \\ 0 \end{pmatrix}.$$

- Similarly, we can represent the incident field for Transverse Magnetic (TM) polarization through

$$\mathbf{H}^i = \mathbf{H}^i(x,z) = \mathbf{B} e^{i\alpha x - i\gamma z}, \quad \mathbf{B} = \begin{pmatrix} 0 \\ B \\ 0 \end{pmatrix}.$$

Light as Electromagnetic Radiation

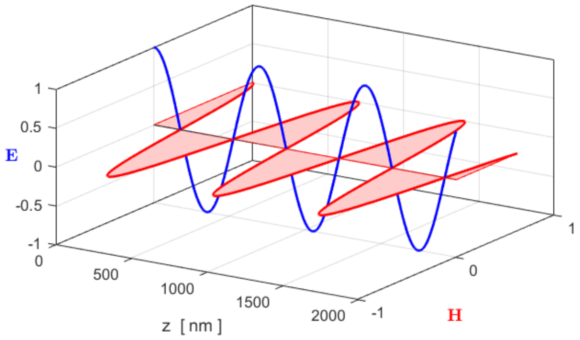

- A light wave is an electromagnetic wave with an electric and a magnetic component. In our model, the electric field **E** oscillates in the vertical direction. The magnetic field **H** is at a right angle to the electric field and oscillates in the horizontal direction. Both are perpendicular to the direction of wave propagation (**z**).

Governing Equations for Layered Media

Under these assumptions, our governing equations are composed of outgoing/bounded solutions of the Helmholtz equation in the upper and lower media

$$\Delta \tilde{u} + (k^u)^2 = 0, \qquad z > g(x), \tag{6a}$$

$$\Delta \tilde{w} + (k^w)^2 = 0, \qquad z < g(x), \tag{6b}$$

$$\tilde{u} - \tilde{w} = -\tilde{u}^i, \qquad z = g(x), \tag{6c}$$

$$\partial_N \tilde{u} - \tau^2 \partial_N \tilde{w} = -\partial_N \tilde{u}^i, \qquad z = g(x). \tag{6d}$$

- $\{\tilde{u}, \tilde{w}\}$ represent the invariant (y) directions of the scattered (electric or magnetic) fields in the upper and lower media.
- $g(x)$ is the grating interface, $\tilde{u}^i$ is the incident radiation.
- $\tau^2 = \begin{cases} 1, & \text{TE}, \\ (k^u/k^w)^2 = (n^u/n^w)^2, & \text{TM}. \end{cases}$
- $k^q, q \in \{u, w\}$ is the wavenumber and n^q is the index of refraction.

Geometry

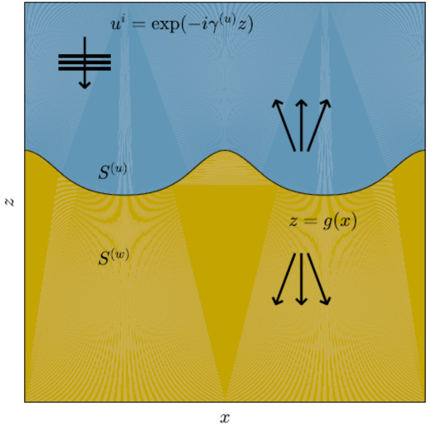

A two-layer structure with a periodic interface, $z = g(x)$, separating two material layers, $S^{(u)}$ and $S^{(w)}$.

- We consider a y–invariant, doubly layered structure.
- The d–periodic interface shape is specified by the graph of the function $z = g(x)$, where $g(x + d) = g(x)$.
- A dielectric (with refractive index n^u) occupies the domain above the interface

$$S^{(u)} := \{z > g(x)\}.$$

- A material of refractive index n^w is in the lower layer

$$S^{(w)} := \{z < g(x)\}.$$

Incident Radiation

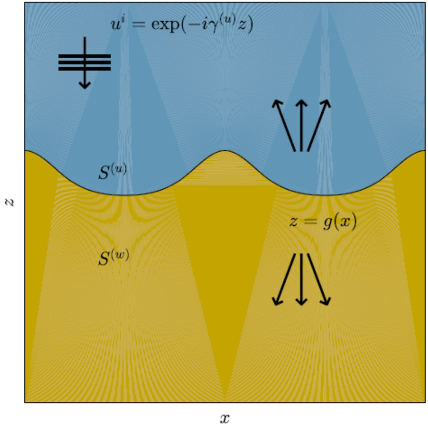

A two-layer structure with a periodic interface, $z = g(x)$, illuminated by plane–wave incidence.

- The structure is illuminated from above by monochromatic plane–wave incident radiation of frequency ω.
- We consider the reduced incident fields

$$\mathbf{E}^i(x,z) = e^{i\omega t}\underline{\mathbf{E}}^i(x,z,t),$$
$$\mathbf{H}^i(x,z) = e^{i\omega t}\underline{\mathbf{H}}^i(x,z,t),$$

  where the time dependence $\exp(-i\omega t)$ is removed.
- The scattered radiation is "outgoing," upward propagating in $S^{(u)}$ and downward propagating in $S^{(w)}$.

Governing Equations Without Phase

- We further factor out the phase $\exp(i\alpha x)$ from the fields $\tilde{u}$ and $\tilde{w}$

$$u(x,z) = e^{-i\alpha x}\tilde{u}(x,z), \quad w(x,z) = e^{-i\alpha x}\tilde{w}(x,z). \tag{7}$$

- Inserting (7) into our governing equations (6) gives outgoing/bounded, d–periodic solutions of

$$\begin{aligned}
&\Delta u + 2i\alpha\partial_x u + (\gamma^u)^2 u = 0, && z > g(x), && \text{(8a)}\\
&\Delta w + 2i\alpha\partial_x w + (\gamma^w)^2 w = 0, && z < g(x), && \text{(8b)}\\
&u - w = \zeta, && z = g(x), && \text{(8c)}\\
&\partial_N u - i\alpha(\partial_x g)u - \tau^2\left[\partial_N w - i\alpha(\partial_x g)w\right] = \psi, && z = g(x). && \text{(8d)}
\end{aligned}$$

- In these, $N = (-\partial_x g, 1)^T$, $\alpha = k^u \sin(\theta)$, and for $q \in \{u, w\}$, $k^q = n^q\omega/c_0 = \omega/c^q$ (c_0 is the speed of light), and $\gamma^q = k^q\cos(\theta)$.

Boundary Conditions

The Dirichlet and Neumann data on the right–hand side of (8c) and (8d) become

$$\zeta(x) := -e^{-i\gamma^u g(x)},$$
$$\psi(x) := (i\gamma^u + i\alpha(\partial_x g))e^{-i\gamma^u g(x)},$$

where $z = g(x)$ is the interfacial surface.

Artificial Boundaries

- We now demonstrate how our scattering problem can be stated in terms of Transparent Boundary Conditions which also truncate the bi–infinite problem domain to one of finite size.
- For this we choose values a and b such that

$$a > |g|_\infty, \quad -b < -|g|_\infty,$$

and define the artificial boundaries $\{z = a\}$ and $\{z = -b\}$.

- In $\{z > a\}$ the Rayleigh expansions tell us that upward propagating solutions of (8a) are

$$u(x,z) = \sum_{p=-\infty}^{\infty} \hat{a}_p e^{i\tilde{p}x + i\gamma_p^u z}. \tag{9}$$

Rayleigh Expansions

- Similarly, downward propagating solutions of (8b) in $\{z < -b\}$ can be expressed as

$$w(x,z) = \sum_{p=-\infty}^{\infty} \hat{d}_p e^{i\tilde{p}x - i\gamma_p^w z}. \tag{10}$$

- Here, $\hat{a}_p$ and $\hat{d}_p$ are known as the upward and downward propagating Rayleigh amplitudes. For $q \in \{u, w\}$ and $p \in \mathbf{Z}$, we define

$$\tilde{p} := \frac{2\pi p}{d}, \quad \alpha_p := \alpha + \tilde{p}, \quad \gamma_p^q := \begin{cases} \sqrt{(k^q)^2 - \alpha_p^2}, & p \in \mathcal{U}^q, \\ i\sqrt{\alpha_p^2 - (k^q)^2}, & p \notin \mathcal{U}^q. \end{cases}$$

Transparent Boundary Conditions

- With these we can define the Transparent Boundary Conditions in the following way: we rewrite (9) as

$$u(x,z) = \sum_{p=-\infty}^{\infty} \left(\hat{a}_p e^{i\gamma_p^u a}\right) e^{i\tilde{p}x + i\gamma_p^u(z-a)} = \sum_{p=-\infty}^{\infty} \hat{\xi}_p e^{i\tilde{p}x + i\gamma_p^u(z-a)}.$$

- We then observe that

$$u(x,a) = \sum_{p=-\infty}^{\infty} \hat{\xi}_p e^{i\tilde{p}x} =: \xi(x).$$

- Also

$$\partial_z u(x,a) = \sum_{p=-\infty}^{\infty} (i\gamma_p^u)\hat{\xi}_p e^{i\tilde{p}x} =: T^u[\xi(x)],$$

which defines the order–one Fourier multiplier T^u.

Transparent Boundary Conditions

- A similar procedure for (10) in the lower field shows that we can write

$$\partial_z w(x,-b) = \sum_{p=-\infty}^{\infty} (-i\gamma_p^w)\hat{\psi}_p e^{i\tilde{p}x} =: T^w[\psi(x)],$$

  which defines the order–one Fourier multiplier T^w.
- From this we state that upward–propagating solutions of (8a) satisfy the Transparent Boundary Condition at $z = a$

$$\partial_z u(x,a) - T^u[u(x,a)] = 0, \quad z = a. \tag{11}$$

- Similarly, downward–propagating solutions of (8b) satisfy the Transparent Boundary Condition at $z = -b$

$$\partial_z w(x,-b) - T^w[w(x,-b)] = 0, \quad z = -b. \tag{12}$$

Full Governing Equations

With these we now state the full set of governing equations as

$$\Delta u + 2i\alpha\partial_x u + (\gamma^u)^2 u = 0, \qquad z > g(x), \tag{13a}$$

$$\Delta w + 2i\alpha\partial_x w + (\gamma^w)^2 w = 0, \qquad z < g(x), \tag{13b}$$

$$u - w = \zeta, \qquad z = g(x), \tag{13c}$$

$$\partial_N u - i\alpha(\partial_x g)u - \tau^2 [\partial_N w - i\alpha(\partial_x g)w] = \psi, \qquad z = g(x), \tag{13d}$$

$$\partial_z u(x, a) - T^u[u(x, a)] = 0, \qquad z = a, \tag{13e}$$

$$\partial_z w(x, -b) - T^w[w(x, -b)] = 0, \qquad z = -b, \tag{13f}$$

$$u(x + d, z) = u(x, z), \tag{13g}$$

$$w(x + d, z) = w(x, z). \tag{13h}$$

Domain Decomposition Method

- In order to take advantage of Dirichlet–Neumann Operators (DNOs), we will rewrite our governing equations (13) in terms of *surface* quantities via a Non–Overlapping Domain Decomposition Method.
- For this we define

$$U(x) := u(x, g(x)), \quad \tilde{U}(x) := -\partial_N u(x, g(x)),$$
$$W(x) := w(x, g(x)), \quad \tilde{W}(x) := \partial_N w(x, g(x)),$$

where u is a d–periodic solution of (13a) and (13e), and w is a d–periodic solution of (13b) and (13f).

- In terms of these our full governing equations (13) are equivalent to the pair of boundary conditions, (13c) & (13d),

$$U - W = \zeta, \quad -\tilde{U} - (i\alpha)(\partial_x g)U - \tau^2 \left[\tilde{W} - (i\alpha)(\partial_x g)W \right] = \psi.$$

Domain Decomposition Method

- Recalling our full governing equations (13) are equivalent to the pair of boundary conditions, (13c) & (13d),

$$U - W = \zeta,$$
$$-\tilde{U} - (i\alpha)(\partial_x g)U - \tau^2 \left[\tilde{W} - (i\alpha)(\partial_x g)W\right] = \psi.$$

- The set of two equations and four unknowns can be closed by noting that the pairs $\{U, \tilde{U}\}$ and $\{W, \tilde{W}\}$ are connected, e.g., by Dirichlet–Neumann Operators (DNOs)

$$G : U \to \tilde{U}, \quad J : W \to \tilde{W}.$$

- These are well–defined operators for sufficiently smooth g (e.g., $g \in C^2$).

Interfacial Reformulation

- We now focus on the interfacial reformulation of our governing equations
$$\mathbf{A}\mathbf{V} = \mathbf{R}. \tag{14}$$
- By the definition of the DNOs
$$\mathbf{A} = \begin{pmatrix} I & -I \\ G + (\partial_x g)(i\alpha) & \tau^2 J - \tau^2 (\partial_x g)(i\alpha) \end{pmatrix}, \tag{15a}$$
$$\mathbf{V} = \begin{pmatrix} U \\ W \end{pmatrix}, \quad \mathbf{R} = \begin{pmatrix} \zeta \\ -\psi \end{pmatrix}. \tag{15b}$$
- The flat–interface version of (15) is $\mathbf{A}_{0,0}\mathbf{V}_{0,0} = \mathbf{R}_{0,0}$ where
$$\mathbf{A}_{0,0} = \begin{pmatrix} I & -I \\ -G_{0,0} & -\tau^2 J_{0,0} \end{pmatrix}, \quad \mathbf{V}_{0,0} = \begin{pmatrix} U_{0,0} \\ W_{0,0} \end{pmatrix}, \quad \mathbf{R}_{0,0} = \begin{pmatrix} \zeta_{0,0} \\ -\psi_{0,0} \end{pmatrix}. \tag{16}$$

Numerical Methods

- A variety of numerical algorithms have been devised for the simulation of these problems including Finite Difference, Finite Element, and Spectral Element methods.
- These methods suffer from the requirement that they discretize the full volume of the problem domain.
- We advocate the use of surface methods, especially the High-Order Perturbation of Surfaces (HOPS) methods:
  - provide the solution at the interface.
  - only discretize the layer interfaces.
  - invert a sparse operator at every wavenumber.
  - are highly accurate, rapid, and robust.
- The HOPS methods are based on the foundational contributions of
  - Field Expansion (FE) method: Bruno & Reitich (1993).
  - Transformed Field Expansion (TFE) method: Nicholls & Reitich (1999).

Boundary and Frequency Perturbations

- Our governing equations are $\mathbf{AV} = \mathbf{R}$ where

$$\mathbf{A} = \begin{pmatrix} I & -I \\ G + (\partial_x g)(i\alpha) & \tau^2 J - \tau^2 (\partial_x g)(i\alpha) \end{pmatrix},$$
$$\mathbf{V} = \begin{pmatrix} U \\ W \end{pmatrix}, \quad \mathbf{R} = \begin{pmatrix} \zeta \\ -\psi \end{pmatrix}.$$

- We take a perturbative approach which makes two smallness assumptions:
  1. Boundary Perturbation: $g(x) = \varepsilon f(x)$, $\varepsilon \in \mathbf{R}$, $\varepsilon \ll 1$,
  2. Frequency Perturbation: $\omega = (1+\delta)\underline{\omega} = \underline{\omega} + \delta\underline{\omega}$, $\delta \in \mathbf{R}$, $\delta \ll 1$.

High–Order Perturbation of Surfaces

- Provided f is sufficiently smooth, we can show that the *joint* analyticity of the operator $\mathbf{A}$ and function $\mathbf{R}$ with respect to ε and δ which will induce a *jointly* analytic solution, $\mathbf{V}$, of $\mathbf{AV} = \mathbf{R}$.
- All of this can be done in the context of Sobolev space theory.
- In this case we can expand

$$\{\mathbf{A}, \mathbf{V}, \mathbf{R}\}(\varepsilon, \delta) = \sum_{n=0}^{\infty} \sum_{m=0}^{\infty} \{\mathbf{A}_{n,m}, \mathbf{V}_{n,m}, \mathbf{R}_{n,m}\} \varepsilon^n \delta^m. \tag{17}$$

Regular Perturbation Theory

- Consider the fundamental problem of applied mathematics: Solve a system of linear equations

$$\mathbf{A}\mathbf{x} = \mathbf{b}, \quad \mathbf{A} \in \mathbf{R}^{n \times n}, \quad \mathbf{x}, \mathbf{b} \in \mathbf{R}^{n},$$

  where $\mathbf{A}$ is invertible.

- Suppose that $\mathbf{A} = \mathbf{A}(\varepsilon)$ and $\mathbf{b} = \mathbf{b}(\varepsilon)$ for some real parameter ε and, further, that this dependence is real analytic so that

$$\mathbf{A}(\varepsilon) = \sum_{n=0}^{\infty} \mathbf{A}_n \varepsilon^n, \quad \mathbf{b}(\varepsilon) = \sum_{n=0}^{\infty} \mathbf{b}_n \varepsilon^n,$$

  are convergent for ε sufficient small.

Regular Perturbation Theory

- In this case it can be shown that, provided that $\mathbf{A}(0) = \mathbf{A}_0$ is invertible, $\mathbf{x} = \mathbf{x}(\varepsilon)$ is also real analytic, so that

$$\mathbf{x}(\varepsilon) = \sum_{n=0}^{\infty} \mathbf{x}_n \varepsilon^n.$$

- Combining the expansions yields

$$\left(\sum_{n=0}^{\infty} \mathbf{A}_n \varepsilon^n \right) \left(\sum_{m=0}^{\infty} \mathbf{x}_m \varepsilon^m \right) = \left(\sum_{n=0}^{\infty} \mathbf{b}_n \varepsilon^n \right).$$

- At order $\mathcal{O}(\varepsilon^n)$ this becomes

$$\sum_{m=0}^{n} \mathbf{A}_{n-m} \mathbf{x}_m = \mathbf{b}_n.$$

Regular Perturbation Theory

- At order zero we have $\mathbf{A}_0 \mathbf{x}_0 = \mathbf{b}_0$ which has the solution

$$\mathbf{x}_0 = \mathbf{A}_0^{-1} \mathbf{b}_0.$$

- At higher orders we find

$$\mathbf{x}_n = \mathbf{A}_0^{-1} \left(\mathbf{b}_n - \sum_{m=0}^{n-1} \mathbf{A}_{n-m} \mathbf{x}_m \right).$$

- It is clear how one would proceed recursively: Given corrections $\{\mathbf{x}_0, \mathbf{x}_1, \ldots, \mathbf{x}_{n-1}\}$, find $\mathbf{x}_n$ from the above recursion and then approximate

$$\mathbf{x}(\varepsilon) \approx \mathbf{x}^N(\varepsilon) := \sum_{n=0}^{N} \mathbf{x}_n \varepsilon^n.$$

High–Order Perturbation of Surfaces

- We have

$$\{\mathbf{A}, \mathbf{V}, \mathbf{R}\}(\varepsilon, \delta) = \sum_{n=0}^{\infty} \sum_{m=0}^{\infty} \{\mathbf{A}_{n,m}, \mathbf{V}_{n,m}, \mathbf{R}_{n,m}\} \varepsilon^n \delta^m.$$

- Using the above strategy, a straightforward calculation reveals that, at each perturbation order (n, m), we must solve

$$\begin{aligned} \mathbf{A}_{0,0} \mathbf{V}_{n,m} = \mathbf{R}_{n,m} &- \sum_{\ell=0}^{n-1} \mathbf{A}_{n-\ell,0} \mathbf{V}_{\ell,m} - \sum_{r=0}^{m-1} \mathbf{A}_{0,m-r} \mathbf{V}_{n,r} \\ &- \sum_{\ell=0}^{n-1} \sum_{r=0}^{m-1} \mathbf{A}_{n-\ell,m-r} \mathbf{V}_{\ell,r}. \end{aligned} \tag{18}$$

High–Order Perturbation of Surfaces

- A brief inspection of the formulas for **A** and **R** reveals that

$$\mathbf{A}_{0,0} = \begin{pmatrix} I & -I \\ G_{0,0} & \tau^2 J_{0,0} \end{pmatrix}, \tag{19a}$$

$$\mathbf{A}_{n,m} = \begin{pmatrix} 0 & 0 \\ G_{n,m} & \tau^2 J_{n,m} \end{pmatrix} + \delta_{n,1} \left\{ 1 + \delta_{m,1} \right\} (\partial_x f)(i\underline{\alpha}) \begin{pmatrix} 0 & 0 \\ 1 & -\tau^2 \end{pmatrix}, \quad n \neq 0 \text{ or } m \neq 0, \tag{19b}$$

$$\mathbf{R}_{n,m} = \begin{pmatrix} \zeta_{n,m} \\ -\psi_{n,m} \end{pmatrix}. \tag{19c}$$

- $\delta_{n,m}$ is the Kronecker delta function and $\zeta_{n,m}$, $\psi_{n,m}$ are known.
- However, the formulas for the (n,m)–th corrections of the Taylor expansions of the DNOs, G and J, must be simulated numerically.

Transformed Field Expansion (TFE) Method

- To simulate the Taylor expansions of G and J numerically, we advocate the Method of Transformed Field Expansions (TFE).
- For brevity we restrict our attention to the DNO in the upper layer, $\{g(x) < z < a\}$, and note that the considerations for the lower layer are largely the same.
- To begin, we write the upper layer DNO as follows: Given an integer $s \geq 0$, if $g \in C^{s+2}$ the unique d–periodic solution of

$$\Delta u + 2i\alpha\partial_x u + (\gamma^u)^2 u = 0, \qquad g(x) < z < a, \tag{20a}$$
$$u(x, g(x)) = U(x), \qquad z = g(x), \tag{20b}$$
$$\partial_z u(x, a) - T^u[u(x, a)] = 0, \qquad z = a, \tag{20c}$$

defines the Upper Layer Dirichlet–Neumann Operator

$$G(g) : U \to \tilde{U} := -(\partial_N u)(x, g(x)). \tag{21}$$

Transformed Field Expansions (TFE) Method

- The TFE method applies a domain–flattening change of variables prior to perturbation expansion. We introduce the domain–flattening change of variables through the prime notation

$$x' = x, \quad z' = a\left(\frac{z - g(x)}{a - g(x)}\right).$$

- With this we can rewrite the DNO problem, (20), in terms of the transformed field

$$u'(x', z') := u\left(x', \left(\frac{a - g(x')}{a}\right) z' + g(x')\right).$$

Upper Layer DNO

- The upper layer DNO problem (20) becomes (upon dropping primes)

$$\Delta u + 2i\alpha\partial_x u + (\gamma^u)^2 u = F(x,z), \qquad 0 < z < a, \tag{22a}$$
$$u(x,0) = U(x), \qquad z = 0, \tag{22b}$$
$$\partial_z u(x,a) - T^u[u(x,a)] = J(x), \qquad z = a, \tag{22c}$$

and (21) as

$$G(g)[U] = -\partial_z u(x,0) + H(x). \tag{23}$$

- Following our HOPS philosophy we assume the joint boundary/frequency perturbation

$$g(x) = \varepsilon f(x), \quad \omega = \underline{\omega} + \delta\underline{\omega},$$

and study the effect of this on (22) and (23).

Upper Layer DNO

These become

$$\Delta u + 2i\underline{\alpha}\partial_x u + (\underline{\gamma}^u)^2 u = \tilde{F}(x,z), \qquad 0 < z < a, \tag{24a}$$

$$u(x,0) = U(x), \qquad z = 0, \tag{24b}$$

$$\partial_z u(x,a) - T^u[u(x,a)] = \tilde{J}(x), \qquad z = a, \tag{24c}$$

and

$$G(\varepsilon f)[U] = -\partial_z u(x,0) + \tilde{H}(x). \tag{25}$$

Transformed Field Expansion (TFE) Recursions

- At this point we posit the expansions

$$u(x,z;\varepsilon,\delta) = \sum_{n=0}^{\infty}\sum_{m=0}^{\infty} u_{n,m}(x,z)\varepsilon^n\delta^m, \quad G(\varepsilon,\delta) = \sum_{n=0}^{\infty}\sum_{m=0}^{\infty} G_{n,m}\varepsilon^n\delta^m.$$

- Upon inserting these into (24) and (25), we find

$$\Delta u_{n,m} + 2i\underline{\alpha}\partial_x u_{n,m} + (\underline{\gamma}^u)^2 u_{n,m} = \tilde{F}_{n,m}(x,z), \quad 0 < z < a, \quad (26a)$$

$$u_{n,m}(x,0) = \delta_{n,0}\delta_{m,0}U(x), \quad z = 0, \quad (26b)$$

$$\partial_z u_{n,m}(x,a) - T^u[u_{n,m}(x,a)] = \tilde{J}_{n,m}(x), \quad z = a, \quad (26c)$$

and

$$G_{n,m}(f) = -\partial_z u_{n,m}(x,0) + \tilde{H}_{n,m}(x). \quad (27)$$

$\tilde{F}_{n,m}$

After a bit of work, one finds that $\tilde{F}_{n,m}$ becomes

$$\begin{aligned}
\tilde{F}_{n,m} = & -\text{div}\left[A_1(f)\nabla u_{n-1,m}\right] - \text{div}\left[A_2(f)\nabla u_{n-2,m}\right] \\
& - B_1(f)\nabla u_{n-1,m} - B_2(f)\nabla u_{n-2,m} \\
& - 2i\underline{\alpha}\partial_x u_{n,m-1} - (\underline{\gamma}^u)^2 u_{n,m-2} - 2(\underline{\gamma}^u)^2 u_{n,m-1} \\
& - 2iS_1(f)\underline{\alpha}\partial_x u_{n-1,m} - 2iS_1(f)\underline{\alpha}\partial_x u_{n-1,m-1} - S_1(f)(\underline{\gamma}^u)^2 u_{n-1,m-2} \\
& - 2S_1(f)(\underline{\gamma}^u)^2 u_{n-1,m-1} - S_1(f)(\underline{\gamma}^u)^2 u_{n-1,m} \\
& - 2iS_2(f)\underline{\alpha}\partial_x u_{n-2,m} - 2iS_2(f)\underline{\alpha}\partial_x u_{n-2,m-1} - S_2(f)(\underline{\gamma}^u)^2 u_{n-2,m-2} \\
& - 2S_2(f)(\underline{\gamma}^u)^2 u_{n-2,m-1} - S_2(f)(\underline{\gamma}^u)^2 u_{n-2,m}.
\end{aligned}$$

$\tilde{J}_{n,m}(x)$ and $\tilde{H}_{n,m}(x)$

Also,

$$\tilde{J}_{n,m} = -\frac{1}{a} f(x) T^u \left[u_{n-1,m}(x,a) \right],$$

and

$$\tilde{H}_{n,m} = (\partial_x f) \partial_x u_{n-1,m}(x,0) + \frac{f}{a} G_{n-1,m}(f)[U] - \frac{f(\partial_x f)}{a} \partial_x u_{n-2,m}(x,0) \\ - (\partial_x f)^2 \partial_z u_{n-2,m}(x,0).$$

A_j, B_j, and S_j

In $\tilde{F}_{n,m}$ the forms for the A_j, B_j, and S_j are

$$A_0 = \begin{pmatrix} 1 & 0 \\ 0 & 1 \end{pmatrix},$$
$$A_1(f) = \frac{1}{a}\begin{pmatrix} -2f & -(a-z)(\partial_x f) \\ -(a-z)(\partial_x f) & 0 \end{pmatrix},$$
$$A_2(f) = \frac{1}{a^2}\begin{pmatrix} f^2 & (a-z)f(\partial_x f) \\ (a-z)f(\partial_x f) & (a-z)^2(\partial_x f)^2 \end{pmatrix},$$

and

$$B_1(f) = \frac{1}{a}\begin{pmatrix} \partial_x f \\ 0 \end{pmatrix}, \quad B_2(f) = \frac{1}{a^2}\begin{pmatrix} -f(\partial_x f) \\ -(a-z)(\partial_x f)^2 \end{pmatrix},$$

and

$$S_0 = 1, \quad S_1(f) = -\frac{2}{a}f, \quad S_2(f) = \frac{1}{a^2}f^2.$$

Numerical Implementation

- Our formulation of the scattering problem is

$$\mathbf{A}(\varepsilon,\delta)\mathbf{V}(\varepsilon,\delta) = \mathbf{R}(\varepsilon,\delta),$$

  and our HOPS approach asks for the joint expansion of the $\{\mathbf{A}, \mathbf{V}, \mathbf{R}\}$ in Taylor series.

- In our approximation we begin by truncating the Taylor series

$$\begin{aligned}\{\mathbf{A}, \mathbf{V}, \mathbf{R}\}(\varepsilon,\delta) &\approx \{\mathbf{A}^{N,M}, \mathbf{V}^{N,M}, \mathbf{R}^{N,M}\}(\varepsilon,\delta) \\ &:= \sum_{n=0}^{N}\sum_{m=0}^{M}\{\mathbf{A}_{n,m}, \mathbf{V}_{n,m}, \mathbf{R}_{n,m}\}\varepsilon^n\delta^m,\end{aligned} \tag{28}$$

  and all that remains is to specify (i.) how the forms $\mathbf{A}_{n,m}$ and $\mathbf{R}_{n,m}$ are simulated, and (ii.) how the operator $\mathbf{A}_{0,0}$ is to be inverted.

The Operator $\mathbf{A}_{0,0}$

- For the latter we note that $\mathbf{A}_{0,0}$ is diagonalized by the Fourier transform so that $\mathbf{A}_{0,0}\mathbf{V}_{n,m} = \mathbf{Q}_{n,m}$ can be expressed as

$$\sum_{p=-\infty}^{\infty} \widehat{\mathbf{A}}_{0,0}(p)\widehat{\mathbf{V}}_{n,m}(p)e^{i\tilde{p}x} = \sum_{p=-\infty}^{\infty} \widehat{\mathbf{Q}}_{n,m}(p)e^{i\tilde{p}x},$$

  which implies

$$\widehat{\mathbf{V}}_{n,m}(p) = \left[\widehat{\mathbf{A}}_{0,0}(p)\right]^{-1} \widehat{\mathbf{Q}}_{n,m}(p).$$

- It is not difficult to see that

$$\widehat{\mathbf{A}}_{0,0}(p) = \begin{pmatrix} 1 & -1 \\ (-i\gamma_p^u) & \tau^2(-i\gamma_p^w) \end{pmatrix},$$

  implying

$$\left[\widehat{\mathbf{A}}_{0,0}(p)\right]^{-1} = \frac{1}{\Delta_p} \begin{pmatrix} \tau^2(-i\gamma_p^w) & 1 \\ (i\gamma_p^u) & 1 \end{pmatrix}, \quad \Delta_p := -(i\gamma_p^u + \tau^2(i\gamma_p^w)).$$

Numerical Results

- Regarding the forms $\mathbf{A}_{n,m}$ and $\mathbf{R}_{n,m}$, these boil down to the (n, m)–th corrections of the DNOs G and J, respectively, in a Taylor series expansion of each jointly in ε and δ. We will simulate these numerically.
- We are now in a position to test a numerical implementation of our method.
- Regarding the algorithm, our HOPS scheme is a High–Order Spectral method in the same spirit as our related Transformed Field Expansion (TFE) algorithm, where nonlinearities are approximated with convolutions implemented via the fast Fourier transform (FFT) algorithm.

A Fourier/Chebyshev Collocation Discretization

- Focusing on the upper layer DNO, G, we begin by approximating

$$u(x,z;\varepsilon,\delta) \approx u^{N,M}(x,z;\varepsilon,\delta) := \sum_{n=0}^{N}\sum_{m=0}^{M} u_{n,m}(x,z)\varepsilon^n\delta^m.$$

- Each of these $u_{n,m}(x,z)$ are then simulated by a Fourier–Chebyshev approach which posits the form

$$u_{n,m}(x,z) \approx u_{n,m}^{N_x,N_z}(x,z) := \sum_{p=-N_x/2}^{N_x/2-1}\sum_{\ell=0}^{N_z} \hat{u}_{n,m,p,\ell} e^{i\tilde{p}x} T_\ell\left(\frac{2z-a}{a}\right),$$

where T_ℓ is the ℓ–th Cheybshev polynomial. The unknowns, $\hat{u}_{n,m,p,\ell}$ are recovered by the collocation approach.

A Fourier/Chebyshev Collocation Discretization

- As mentioned previously, the Fourier–Chebyshev approach posits the form

$$u_{n,m}(x,z) \approx u_{n,m}^{N_x,N_z}(x,z) := \sum_{p=-N_x/2}^{N_x/2-1} \sum_{\ell=0}^{N_z} \hat{u}_{n,m,p,\ell} e^{i\tilde{p}x} T_\ell \left(\frac{2z-a}{a} \right).$$

- More specifically, our HOPS/TFE algorithm requires $N_x \times N_z$ unknowns at every perturbation order, (n, m).
- As our problem is x–periodic, we will expand using a Fourier spectral method in the lateral direction where we require N_x equally–spaced gridpoints.
- However, our problem is not z–periodic, so our strategy is to use a Chebyshev spectral method in the vertical direction. For this, we select N_z collocation points.

A Fourier/Chebyshev Collocation Discretization

- With this we can simulate the upper layer DNO through

$$G(x;\varepsilon,\delta) \approx G^{N,M}(x;\varepsilon,\delta) := \sum_{n=0}^{N}\sum_{m=0}^{M} G_{n,m}(x)\varepsilon^n\delta^m.$$

- In this

$$G_{n,m}(x) \approx G_{n,m}^{N_x}(x) := \sum_{p=-N_x/2}^{N_x/2-1} \hat{G}_{n,m,p} e^{i\tilde{p}x}, \tag{29}$$

and the $\hat{G}_{n,m,p}$ are recovered from the $\hat{u}_{n,m,p,\ell}$.

The Reflectivity Map

- Previously, we observed that solutions to the Helmholtz problem in the upper layer can be expressed in terms of Rayleigh expansions

$$u(x,z) = \sum_{p=-\infty}^{\infty} \hat{a}_p e^{i\tilde{p}x + i\gamma_p^u z}. \tag{30}$$

- For $q \in \{u, w\}$ and $p \in \mathbf{Z}$, we defined

$$\tilde{p} := \frac{2\pi p}{d}, \quad \alpha_p := \alpha + \tilde{p}, \quad \gamma_p^q := \begin{cases} \sqrt{(k^q)^2 - \alpha_p^2}, & p \in \mathcal{U}^q, \\ i\sqrt{\alpha_p^2 - (k^q)^2}, & p \notin \mathcal{U}^q, \end{cases}$$

- Regarding the solution (30) we note the very different character of the solution for wavenumbers p in the set

$$\mathcal{U}^u := \left\{ p \in \mathbf{Z} \mid \alpha_p^2 < (k^u)^2 \right\},$$

and those that are not.

The Reflectivity Map

- Components of $u(x, z)$ corresponding to $p \in \mathcal{U}^u$ propagate away from the layer interface, while those not in this set decay exponentially from $z = g(x)$.
- The latter are called evanescent waves while the former are propagating (defining the set of propagating modes $\mathcal{U}^u$) and carry energy away from the grating.
- With this in mind one defines the efficiencies

$$e_p^u := (\gamma_p^u / \gamma^u) \left| \hat{a}_p \right|^2, \quad p \in \mathcal{U}^u,$$

- and the Reflectivity Map as the sum of efficiencies in the upper layer

$$R := \sum_{p \in \mathcal{U}^u} e_p^u. \tag{31}$$

The Reflectivity Map

- Similar quantities can be defined in the lower layer, and with these the principle of conservation of energy can be stated for structures composed entirely of dielectrics

$$\sum_{p \in \mathcal{U}^u} e_p^u + \tau^2 \sum_{p \in \mathcal{U}^w} e_p^w = 1.$$

- In this situation a useful diagnostic of convergence for a numerical scheme is the "Energy Defect"

$$D := 1 - \sum_{p \in \mathcal{U}^u} e_p^u - \tau^2 \sum_{p \in \mathcal{U}^w} e_p^w, \qquad (32)$$

which should be zero for a purely dielectric structure.

Simulation: Reflectivity Map for Vacuum over Dielectric

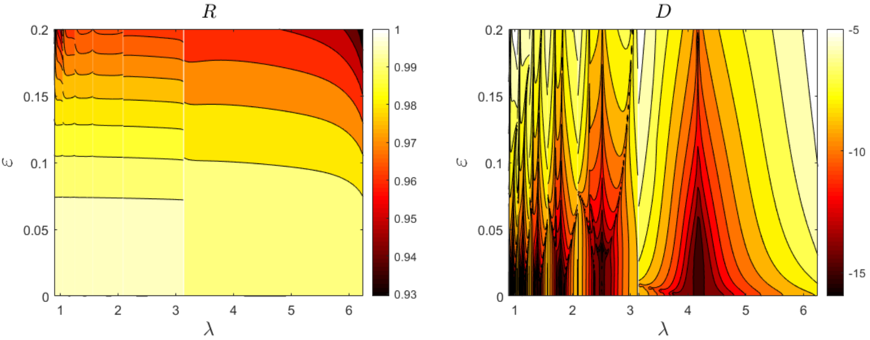

Figure 1: The Reflectivity Map, $R(\varepsilon, \delta)$, and energy defect D computed with our HOPS algorithm with Taylor summation. We set $N = M = 16$ and the parameter choices were $\alpha = 0$, $n^u = 1$, and $n^w = 1.1$.

Simulation: Reflectivity Map for Vacuum over Dielectric with Nonzero Alpha

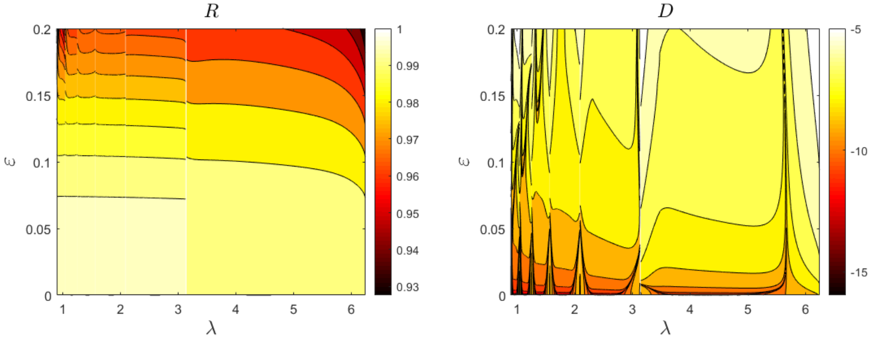

Figure 2: The Reflectivity Map, $R(\varepsilon, \delta)$, and energy defect D computed with our HOPS algorithm with Taylor summation. We set $N = M = 16$ and the parameter choices were $\alpha = 0.01$, $n^u = 1$, and $n^w = 1.1$.

Simulation: Reflectivity Map for Vacuum over Silver and Gold

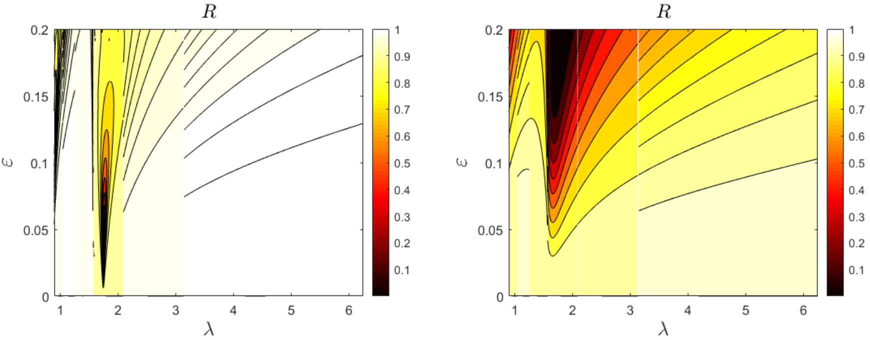

Figure 3: The Reflectivity Map, $R(\varepsilon, \delta)$, for silver (left) and gold (right) with Padé summation. We set $N = M = 15$ and parameter choices were $\alpha = 0$, $n^u = 1$, $n^w = 0.05 + 2.275i$ (left) and $n^w = 1.48 + 1.883i$ (right).

Simulation: Reflectivity Map for Non–Physical Dielectric Constants

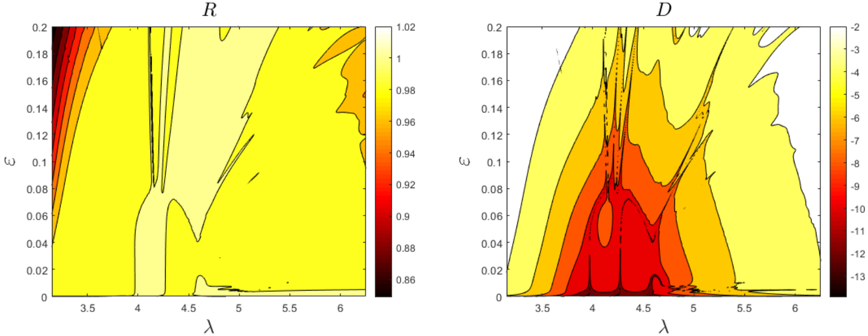

Figure 4: The Reflectivity Map, $R(\varepsilon, \delta)$, and energy defect D computed with our HOPS algorithm with Padé summation. We set $N = M = 15$ and parameter choices were $\alpha = 0.1$, $n^u = 15$, and $n^w = 20i$.

Simulation: Reflectivity Map for Non–Physical Dielectric Constants

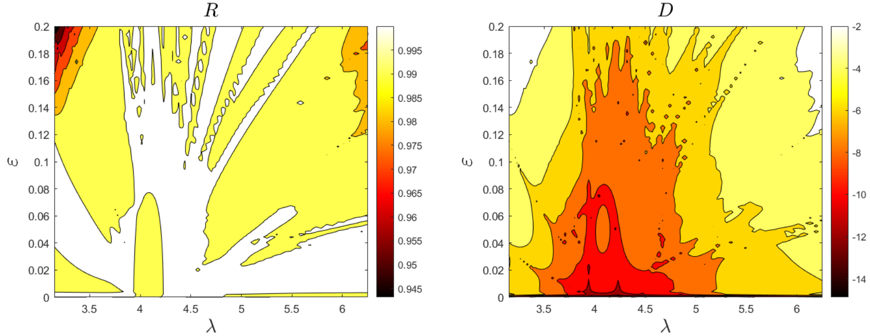

Figure 5: The Reflectivity Map, $R(\varepsilon, \delta)$, and energy defect D computed with our HOPS algorithm with Padé summation. We set $N = M = 20$ and parameter choices were $\alpha = 0.1$, $n^u = 10$, and $n^w = 40i$.

Future Work

1. Extend HOPS algorithm to multilayered surfaces with different material layers. Introduce a new DNO to handle the intermediate layers.
2. Implement parallel programming techniques to handle the computation of the intermediate layers.
3. Introduce multiple small perturbation parameters outside of an interfacial perturbation (ε) and the frequency perturbation (δ). Extend the proof of analyticity to handle any finite number of perturbation parameters.
4. Develop techniques to expand around Rayleigh singularities where the Taylor series expansion is invalid.